

# CNO and *pep* neutrino spectroscopy in Borexino: Measurement of the deep underground production of cosmogenic $^{11}\text{C}$ in organic liquid scintillator

H. Back,<sup>1,\*</sup> M. Balata,<sup>2</sup> G. Bellini,<sup>3</sup> J. Benziger,<sup>4</sup> S. Bonetti,<sup>3</sup> B. Caccianiga,<sup>3</sup> F. Calaprice,<sup>4</sup> D. D'Angelo,<sup>5,†</sup> A. de Bellefon,<sup>6</sup> H. de Kerret,<sup>6</sup> A. Derbin,<sup>7</sup> A. Etenko,<sup>8</sup> R. Ford,<sup>4</sup> D. Franco,<sup>3,9,‡</sup> C. Galbiati,<sup>4</sup> S. Gazzana,<sup>2</sup> M. Giammarchi,<sup>3</sup> A. Goretti,<sup>4</sup> C. Grieb,<sup>1</sup> E. Harding,<sup>4</sup> G. Heusser,<sup>9</sup> A. Ianni,<sup>2</sup> A. M. Ianni,<sup>4</sup> V. V. Kobychev,<sup>10</sup> G. Korga,<sup>3</sup> Y. Kozlov,<sup>8</sup> D. Kryn,<sup>6</sup> M. Laubenstein,<sup>2</sup> C. Lendvai,<sup>5</sup> M. Leung,<sup>4</sup> E. Litvinovich,<sup>8</sup> P. Lombardi,<sup>3</sup> I. Machulin,<sup>8</sup> J. Maneira,<sup>3,11,§</sup> D. Manuzio,<sup>12</sup> G. Manuzio,<sup>12</sup> F. Masetti,<sup>13</sup> U. Mazzucato,<sup>13</sup> K. McCarty,<sup>4</sup> E. Meroni,<sup>3</sup> L. Miramonti,<sup>3</sup> M. E. Monzani,<sup>2</sup> V. Muratova,<sup>7</sup> L. Niedermeier,<sup>5</sup> L. Oberauer,<sup>5</sup> M. Obolensky,<sup>6</sup> F. Ortica,<sup>13</sup> M. Pallavicini,<sup>12</sup> L. Papp,<sup>3</sup> L. Perasso,<sup>3</sup> A. Pocar,<sup>4</sup> R. S. Raghavan,<sup>1</sup> G. Ranucci,<sup>3</sup> A. Razeto,<sup>2</sup> A. Sabelnikov,<sup>2</sup> C. Salvo,<sup>12</sup> S. Schoenert,<sup>9</sup> T. Shutt,<sup>14</sup> H. Simgen,<sup>9</sup> M. Skorokhvatov,<sup>8</sup> O. Smirnov,<sup>7</sup> A. Sotnikov,<sup>7</sup> S. Sukhotin,<sup>8</sup> Y. Suvorov,<sup>2</sup> V. Tarasenkov,<sup>8</sup> R. Tartaglia,<sup>2</sup> D. Vignaud,<sup>6</sup> R. B. Vogelaar,<sup>1</sup> F. Von Feilitzsch,<sup>5</sup> V. Vyrodov,<sup>8</sup> M. Wójcik,<sup>15</sup> O. Zaimidoroga,<sup>7</sup> and G. Zuzel<sup>9</sup>

<sup>1</sup>Physics Department, Virginia Polytechnic Institute and State University, Robeson Hall, Blacksburg, VA 24061-0435, USA

<sup>2</sup>I.N.F.N. Laboratori Nazionali del Gran Sasso, SS 17 bis Km 18+910, I-67010 Assergi(AQ), Italy

<sup>3</sup>Dipartimento di Fisica Università and I.N.F.N., Milano, Via Celoria, 16 I-20133 Milano, Italy

<sup>4</sup>Dept. of Physics, Princeton University, Jadwin Hall, Washington Rd, Princeton NJ 08544-0708, USA

<sup>5</sup>Technische Universität München, James Franck Strasse, E15 D-85747, Garching, Germany

<sup>6</sup>Astroparticule et Cosmologie APC, Collège de France, 11 place Marcelin Berthelot, 75231 Paris Cedex 05, France

<sup>7</sup>Joint Institute for Nuclear Research, 141980 Dubna, Russia

<sup>8</sup>RRC Kurchatov Institute, Kurchatov Sq.1, 123182 Moscow, Russia

<sup>9</sup>Max-Planck-Institut fuer Kernphysik, Postfach 103 980 D-69029, Heidelberg, Germany

<sup>10</sup>Kiev Institute for Nuclear Research, 29 Prospekt Nauki 06380 Kiev, Ukraine

<sup>11</sup>Queen's University, Physics Department, Kingston, Ontario, Canada K7L 3N6

<sup>12</sup>Dipartimento di Fisica Università and I.N.F.N., Genova, Via Dodecaneso, 33 I-16146 Genova, Italy

<sup>13</sup>Dipartimento di Chimica Università, Perugia, Via Elce di Sotto, 8 I-06123, Perugia, Italy

<sup>14</sup>Case Western Reserve University, Cleveland OH 44118, USA

<sup>15</sup>M.Smoluchowski Institute of Physics, Jagellonian University, PL-30059 Krakow, Poland

(Dated: November 5, 2013)

Borexino is an experiment for low energy neutrino spectroscopy at the Gran Sasso underground laboratories. It is designed to measure the mono-energetic  $^7\text{Be}$  solar neutrino flux in real time, via neutrino-electron elastic scattering in ultra-pure organic liquid scintillator. Borexino has the potential to also detect neutrinos from the *pep* fusion process and the CNO cycle. For this measurement to be possible, radioactive contamination in the detector must be kept extremely low. Once sufficiently clean conditions are met, the main background source is  $^{11}\text{C}$ , produced in reactions induced by the residual cosmic muon flux on  $^{12}\text{C}$ . In the process, a free neutron is almost always produced.  $^{11}\text{C}$  can be tagged on an event by event basis by looking at the three-fold coincidence with the parent muon track and the subsequent neutron capture on protons. This coincidence method has been implemented on the Borexino Counting Test Facility data. We report on the first event by event identification of *in situ* muon induced  $^{11}\text{C}$  in a large underground scintillator detector. We measure a  $^{11}\text{C}$  production rate of  $0.130 \pm 0.026$  (stat)  $\pm 0.014$  (syst)  $\text{day}^{-1} \text{ton}^{-1}$ , in agreement with predictions from both experimental studies performed with a muon beam on a scintillator target and *ab initio* estimations based on the  $^{11}\text{C}$  producing nuclear reactions.

PACS numbers: 25.20.-x; 25.30.Mr; 26.65.+t; 28.20.Gd; 96.50.S-; 96.60.-j

Keywords: Muon-induced nuclear reactions; Photonuclear reactions; Solar neutrinos; Low background experiments; Borexino

## I. INTRODUCTION

Results from solar neutrino [1] and reactor [2] antineutrino experiments provide compelling evidence for neutrino oscillations as the explanation of the long-standing solar neutrino

problem [3]. The next goal in solar neutrino physics is probing in real time the low energy ( $< 2$  MeV) component of the solar neutrino spectrum, which accounts for more than 99% of the total flux. This includes neutrinos produced in the *pp*,  $^7\text{Be}$ , and *pep* nuclear fusion reactions and the CNO-cycle. Particularly, *pep* and CNO neutrinos are an ideal source for probing the energy region, between 1 and 3 MeV, at which the transition between matter and vacuum dominated oscillations is supposed to occur, according to the MSW-LMA oscillation solution [4]. Furthermore, the *pep* and *pp* solar neutrino rates are directly related, via the ratio of the cross section of the two reactions. Measuring the *pep* neutrino flux is hence a way to study the fundamental *pp* fusion reaction by which the Sun

\*Present address: North Carolina State University, 890 Oval Drive, Campus Box 8206, Raleigh, NC 27695-8206, USA

†Electronic address: Davide.Dangelo@lngs.infn.it

‡Electronic address: Davide.Franco@mi.infn.it

§Present address: Laboratório de Instrumentação e Física Experimental de Partículas (LIP), Av. Elias Garcia, 14, 1°, 1000-149 Lisboa, Portugal.

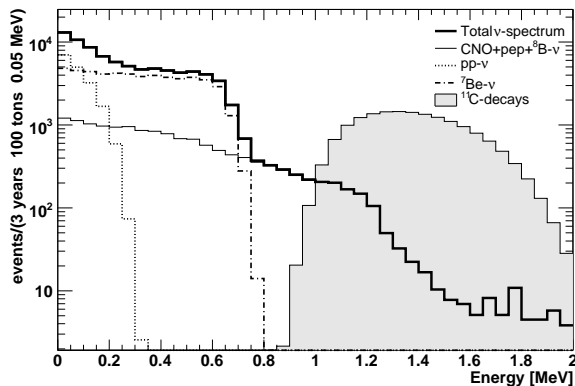


FIG. 1: Expected recoil electron energy for different solar neutrinos interacting in Borexino assuming 3 year live time exposure, 100 tons fiducial volume and a detector energy resolution of  $5\%/\sqrt{E_{[MeV]}}$ . Neutrino fluxes are derived assuming the Standard Solar Model BP2004+LUNA [18, 19] and the LMA oscillation scenario [20]. The shaded superimposed area is the expected  $^{11}\text{C}$  background [10].

burns, and improves our knowledge of the solar neutrino luminosity, thence yielding a crucial check of the Sun stability over a time scale of  $10^5 - 10^6$  years by comparison with the photon luminosity. CNO neutrinos play a key role on the age estimation of the Globular Clusters [5], pivotal in setting a lower limit for the age of the universe.

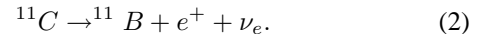
Deep underground organic liquid scintillator detectors, like Borexino and KamLAND, are well positioned to measure *pep* and CNO solar neutrinos. The 1.4 MeV, mono-energetic *pep* neutrinos are particularly well identifiable by the characteristic Compton-like electron recoil spectrum they produce. The main challenge they face is the identification and suppression of the  $^{11}\text{C}$  background.  $^{11}\text{C}$  is produced deep underground by residual cosmic muons interacting with  $^{12}\text{C}$  atoms in the scintillator. The rate of the process is a function of the location and depth of the experiment. As can be seen in fig. 1, the  $^{11}\text{C}$  background at Gran Sasso falls in the energy region for the detection of *pep* and CNO neutrinos. In 1996, Deutsch [6] suggested that  $^{11}\text{C}$  decays could be detected and subtracted exploiting the neutron emission in the reaction:

$$\mu (+ \text{secondaries}) + ^{12}\text{C} \rightarrow \mu (+ \text{secondaries}) + ^{11}\text{C} + n. \quad (1)$$

He proposed using a three-fold coincidence which links the parent muon, the neutron capture on protons, and the  $^{11}\text{C}$  decay. The validity of such technique was studied in detail in [7]. We apply the three-fold coincidence technique to data from the Borexino Counting Test Facility (CTF). This is, to the best of our knowledge, the first *in situ* event by event detection of  $^{11}\text{C}$  production deep underground. We then use our results to evaluate *pep* solar neutrino detection with Borexino.

## II. $^{11}\text{C}$ IN SITU PRODUCTION: THE THREE-FOLD COINCIDENCE TECHNIQUE

$^{11}\text{C}$   $\beta^+$ -decays with a mean life of 29.4 min and an end-point energy of 0.96 MeV:



The total energy released in the detector by the decay and the following positron annihilation is between 1.02 and 1.98 MeV, partially covering the best window for the observation of the *pep*+CNO signal (0.8-1.3 MeV).

The probability to produce  $^{11}\text{C}$  nuclides in muon-induced cascades was experimentally determined with a target experiment (NA54) on a muon beam at CERN [10]. The inferred  $^{11}\text{C}$  rate for Borexino and CTF is  $0.146 \pm 0.015 \text{ day}^{-1} \text{ ton}^{-1}$  ( $0.074 \pm 0.008 \text{ day}^{-1} \text{ ton}^{-1}$  in the *pep*+CNO neutrino window).

The study reported in [7] identified eight different processes for the  $^{11}\text{C}$  production in muon showers and provided a quantitative estimate for the rate in all the production channels. The result seems robust in view of the fact that the calculated production rate matches the rate measured at the NA54 CERN facility.

Two of the production channels identified,  $^{12}\text{C}(p,d)^{11}\text{C}$  and  $^{12}\text{C}(\pi^+, \pi^0+p)^{11}\text{C}$ , do not produce a free neutron in the final state, and therefore escape any possibility of detection by the three-fold coincidence technique. These two production channels are referred to as "invisible channels", and they account for 5% of the  $^{11}\text{C}$  production rate [7].

Neutrons are captured on hydrogen with a capture mean time of  $\sim 250 \mu\text{s}$  in pseudocumene emitting a characteristic  $\gamma$  of 2.2 MeV. Neutrons can also be captured on carbon isotopes emitting  $\gamma$  with larger energy, but the cross section is two orders of magnitude lower than on hydrogen.

In order to identify and suppress the  $^{11}\text{C}$  background, each 2.2 MeV  $\gamma$  produced in the scintillator from the muon-induced showers must be localized in space and time.

After each muon-induced neutron detection, the three-fold coincidence technique defines a set of potential  $^{11}\text{C}$  candidates within a time delay  $t$  from the detected muon and inside a sphere of radius  $r$  from the neutron capture point. We assume that no convective currents move the  $^{11}\text{C}$  nuclide from the production point in the time scale of the  $^{11}\text{C}$  mean life.

In Borexino, the  $^{11}\text{C}$  candidates will be discarded in order to increase the *pep*+CNO signal to background ratio. The success of the *pep* and CNO neutrino measurement will depend on two main conditions: the minimization of the detector mass-time fraction lost to the cuts implementing the three-fold coincidence and the achievement of a high efficiency in the  $^{11}\text{C}$  suppression.

The limited size of CTF represents a challenging test for the three-fold coincidence technique. The goal in CTF is the measurement of the  $^{11}\text{C}$  production rate by looking at the time profile of the  $^{11}\text{C}$  candidates.

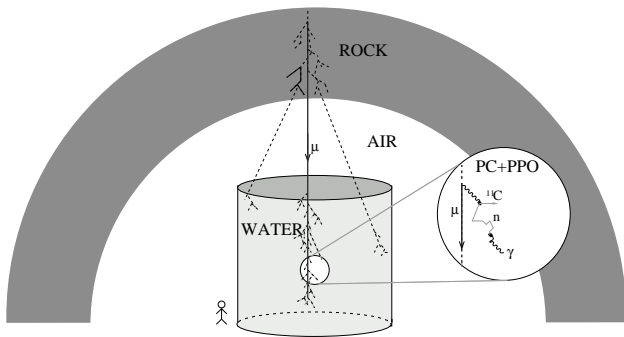


FIG. 2: Overview of the CTF detector and of the physical processes included in the simulation.

### III. EXPERIMENTAL SETUP

CTF [8] is the Borexino prototype detector installed at the Gran Sasso underground laboratory. It was designed to test the required radiopurity of the Borexino liquid scintillator and its purification strategy. The CTF of Borexino was the first detector to prove the level of purities needed for solar neutrino physics on a multiton-scale, in its 1994-95 campaign [9]. The active detector consists of 3.73 tons ( $0.88 \text{ ton/m}^3$  density) of the Borexino-like scintillator, a mixture of pseudocumene (PC, 1,2,4-trimethylbenzene,  $\text{C}_6\text{H}_3(\text{CH}_3)_3$ ) plus 1.5 g/l of PPO (2,5-diphenyloxazole,  $\text{C}_{15}\text{H}_{11}\text{NO}$ ), housed in a 1 m radius transparent nylon vessel. A 7 m diameter stainless steel open structure supports 100 8" photomultiplier tubes (PMT) equipped with light concentrators which provide an optical coverage of 21%.

The detector is housed within a cylindrical tank (11 m diameter and 10 m height) containing 1000 tons of pure water, which provides 4.5 m shielding against neutrons from the rock and external  $\gamma$ -rays from the rock and from the same PMTs. 16 upward-looking PMTs mounted on the bottom of the tank veto muons by detecting the Čerenkov light in water (muon veto system). The veto efficiency is larger than 99.7% for muon shower events with energy  $> 4 \text{ MeV}$ .

A set of analog to digital (ADC) and time to digital (TDC) converters records the charge and time information of the PMT pulses for each event. During the acquisition, a second identical electronic chain is sensitive to the next event occurring within the following 8.3 ms. The electronics can therefore detect pairs of fast time-correlated events. The coincidence time between the two chains is measured by means of a long range TDC. Further events are ignored until the first chain is "re-armed" ( $\sim 20 \text{ ms}$ ). For longer delays the computer clock is used providing an accuracy of  $\sim 50 \text{ ms}$ .

The trigger condition is set by requiring the signal of 6 PMTs over threshold within a time window of 30 ns. The corresponding energy threshold is  $\sim 20 \text{ keV}$  with 50% detection efficiency, while 99% efficiency is reached above 90 keV. The trigger for the second chain is set at a higher value, corresponding to 200 keV (99% efficiency).

The electronic can be also triggered by the so-called *after-pulses* which are spurious pulses following genuine PMT out-

put pulse. To avoid such effect, the second chain is vetoed for  $20 \mu\text{s}$  after an event tagged by the muon veto system.

The energy response of the detector is calibrated run-by-run by using the energy spectrum of  $^{14}\text{C}$  decays, naturally present in the scintillator. The measured light yield is  $\sim 3.6$  photoelectrons per PMT for 1 MeV electrons. The electronics saturate at about 6 MeV.

The position of the interaction vertex is reconstructed by means of a maximum likelihood method exploiting the hit time distribution. The reconstruction algorithm, calibrated by inserting a  $^{222}\text{Rn}$  source in the active volume, provides a resolution of 10 cm at 1 MeV.

### IV. DATA SELECTION

The residual cosmic muon flux at Gran Sasso depth (3800 m.w.e. maximum depth, 3,200 m.w.e. slant depth) has a rate of  $1.2 \text{ m}^{-2} \text{ h}^{-1}$  and an average energy of  $\langle E_\mu \rangle = 320 \pm 4_{stat} \pm 11_{sys} \text{ GeV}$  [12]. The requirements in the selection of cosmic muons are two-fold: they must be tagged by the muon veto and they must saturate the electronics. Cosmic muons, crossing the scintillator, produce enough light to blind the detector.

For each detected muon, we select the following event in the time window  $T_n = [20, 2000] \mu\text{s}$  as a candidate event for a neutron capture  $\gamma$ . The probability that a random event ( $R = 0.04 \text{ s}^{-1}$  rate) is detected instead of the  $2.2 \text{ MeV}$   $\gamma$  has an upper limit equal to  $T_n \times R \sim 8 \times 10^{-5}$ . We measured the mean capture time of neutrons on protons equal to  $257 \pm 27 \mu\text{s}$ , taking into account also events with double neutron emission.

For each muon-gamma coincidence,  $^{11}\text{C}$  candidates are selected in a subsequent time window  $T_w = 300 \text{ min}$ , 10 times the  $^{11}\text{C}$  mean life.

Random coincidences collected in this window are mainly  $^{210}\text{Bi}$  ( $Q_\beta=1.16 \text{ MeV}$ ) and  $^{40}\text{K}$  ( $Q_\beta=1.32 \text{ MeV}$  BR=0.893 and  $Q_{EC}=1.51 \text{ MeV}$  BR=0.107) contamination and external  $\gamma$  radiation, while  $^{214}\text{Bi}$  ( $Q_\beta=3.27 \text{ MeV}$ ) events are discarded through the  $^{214}\text{Bi}$ -Po coincidence.

The time profile of the background is expected to be flat on the scale of 300 minute since the background rate is constant and random coincidences are not correlated with cosmic muons. The only bias is introduced by the end of the data run (typically lasting 2-3 days) which interrupts 8% of the selection windows. In such cases the window is completed to 300 min from a random instant in the run in order to correctly maintain the background time profile flat. We estimated that the correspondent probability to loose a  $^{11}\text{C}$  event is 1% [16].

The definition of the optimal energy range of observation, 1.15-2.25 MeV, to detect the  $^{11}\text{C}$  decays, depends on two main requirements: the enhancement of the signal ( $^{11}\text{C}$  decays) to background (random events) ratio and the minimization of the systematic errors introduced by the energy scale uncertainty. In case  $\gamma$ 's from the positron annihilation escape the vessel and deposit energy in the water buffer, the detected energy of the  $^{11}\text{C}$  decay falls below the observation range. Defining a 0.8 m radius fiducial volume, we reduce non-contained events by a factor 20. Further, the radial cut avoids distorting optical

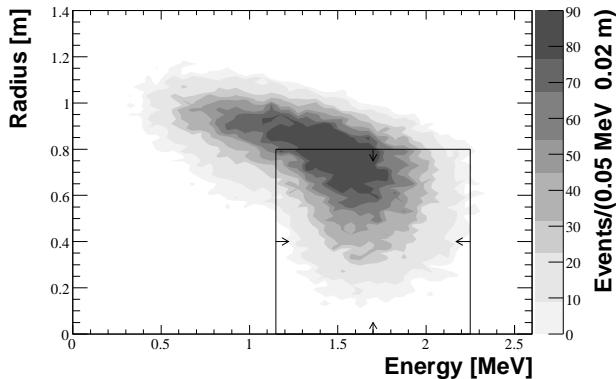


FIG. 3: Scatter plot of the simulated  $^{11}\text{C}$ -decay radial position vs energy. Solid lines represent the cuts applied in the analysis. Events with an energy lower than 1.022 MeV are due to the escaping positron annihilation  $\gamma$ 's.

effects on the border like the total reflection due to the different refractive indexes of the scintillator and the buffer.

The last applied cut exploits the spatial correlation between the  $^{11}\text{C}$  and the neutron capture points. The events are in fact selected in a sphere of radius  $r$  centered on the reconstructed  $2.2\text{MeV}\gamma$ : for  $r = 35\text{ cm}$  the background is suppressed by a factor larger than 20 while the signal is reduced only by a factor  $\sim 2$ .

The efficiencies and optimal parameters of the cuts here discussed have been quoted via the Monte Carlo simulation described in the next section.

## V. THE MONTE CARLO SIMULATION

An accurate quantification of the cut efficiencies requires a full simulation of the  $^{11}\text{C}$  production process from the muon-induced showers originated in the rock to the neutron capture and to the  $^{11}\text{C}$  decay.

The Monte Carlo has been developed in two main steps. First we generated and tracked muons and the subsequent cascades with a FLUKA-based code [13]. The code simulates a 320 GeV muon-beam, downward oriented and uniformly distributed over the entire CTF water tank. At this step, the geometry is simplified to only four volumes: 4 m of rocks ( $\text{CaCO}_3$  and  $\text{MgCO}_3$ ) [14], the air, the water of the CTF tank and finally the scintillator as shown in Figure 2. The purpose of the FLUKA-based simulation code is the generation of neutrons in scintillator and their propagation in the whole detector.

In the second step, an *ad hoc* code, named CTF code [15, 17], generates, tracks and reconstructs  $^{11}\text{C}$  decays and  $2.2\text{MeV}\gamma$ 's from the neutron capture. The coordinates of the neutron production ( $\vec{P}_p$ ) and capture ( $\vec{P}_c$ ) points from the FLUKA output are input parameters in the CTF code:  $\vec{P}_p$  corresponds to the origin of the  $^{11}\text{C}$ -decay while  $\vec{P}_c$  is assumed as the starting position of the  $2.2\text{MeV}\gamma$  produced in

the neutron capture on hydrogen.

The CTF code simulates in detail the detector geometry including the nylon vessel and the phototubes. Each energy deposit is converted into optical photons which are propagated inside the detector until they are absorbed in the detector material or detected on the PMT's.

The tracking code provides a detailed simulation of the main optical processes like the scintillation light production, the absorption and reemission processes in the scintillator and diffusion on the nylon vessel.

After all, the same reconstruction code used in the real data introduces the energy and spatial resolution effects on the simulated ones. The final  $^{11}\text{C}$  radial and energy spectra are shown in figure 3.

The simulated neutron capture mean time,  $254 \pm 1\ \mu\text{s}$ , is in good agreement with the measured one,  $257 \pm 27\ \mu\text{s}$ .

Secondary particles generating a  $^{11}\text{C}$  event without trig-

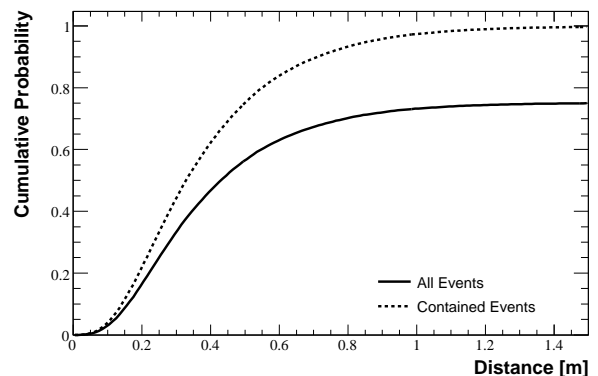


FIG. 4: Cumulative probability to contain a  $^{11}\text{C}$  event in a sphere of radius  $r$  centered on the  $2.2\text{MeV}\gamma$

gering the muon veto have been investigated. From the simulation, we expect mainly  $\gamma$ 's (91.8%) and  $e^+e^-$  pairs (8.1%). Their contribution to the invisible  $^{11}\text{C}$  production rate has been estimated in less than  $5 \times 10^{-4}\ \text{day}^{-1}$  (99.99% C.L.) by convoluting their rates with the  $^{11}\text{C}$  production cross sections [7].

The main inefficiency in the measurement is due to neutrons escaping the vessel. If the neutron, indeed, is captured in water and the subsequent  $\gamma$  does not deposit energy in scintillator, the  $\mu - \gamma_{2.2\text{MeV}}$  coincidence is not triggered and the signal is lost. Neutrons escaping the 1 m CTF vessel account for 26.8%. For  $\sim 50\%$  of the fully contained neutrons, the associated  $^{11}\text{C}$  event falls in a 35 cm radius sphere centered on the reconstructed  $2.2\text{MeV}\gamma$ , as shown in Figure 4.

All the cut efficiencies are quoted in Table I.

## VI. THE DATA ANALYSIS

The analyzed data set corresponds to an effective detector live time of 611 days (June 2002, February 2005).

The time profile of the data sample selected by the three-fold

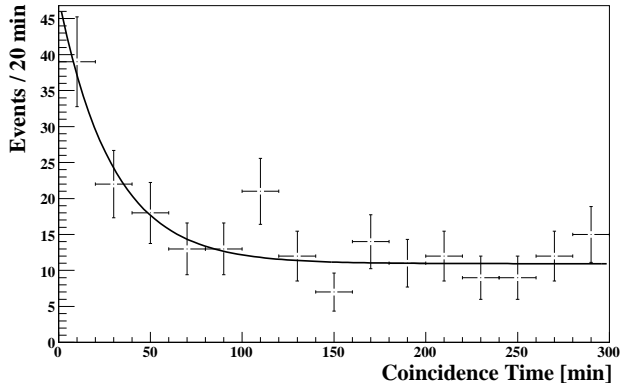


FIG. 5: Fit of the data sample time profile selected by the three-fold coincidence ( $\chi^2/\text{ndf} = 9.7/13$ ) with free parameters  $A$  and  $b$  (see Eq 3).

coincidence technique, shown in Figure 5, is fitted with:

$$P(t) = \frac{A}{\tau} e^{-\frac{t}{\tau}} + b, \quad (3)$$

where the free variables in the fit,  $A$  and  $\tau$ , are the number of  $^{11}\text{C}$  nuclides and the  $^{11}\text{C}$  mean life, respectively. The fit finds  $\tau = 27 \pm 11$  min ( $A = 53 \pm 13$ ,  $b \times T_w = 166 \pm 17$  and  $\chi^2/\text{d.o.f} = 9.7/12$ ) in agreement with the nominal value (29.4 min), proving the robustness of the three-fold coincidence technique. Moreover, if the 300 min window is started independently from the  $\mu - \gamma_{2.2\text{MeV}}$  coincidence, the fit is unable to identify any feature compatible with a decay function.

Performing the fit with  $\tau$  fixed to the nominal value, the  $^{11}\text{C}$

TABLE I: Efficiencies for the  $^{11}\text{C}$  production rate measurement in CTF.

Efficiency Reason	Value
$\varepsilon_{vis}$ visible channels	0.955
$\varepsilon_{end}$ end of run	0.990
$\varepsilon_t$ $\mu$ -2.2MeV $\gamma$ coincidence	0.925
$\varepsilon_{escape}$ contained neutrons	0.732
$\varepsilon_c$ $^{11}\text{C}$ energy $E \in [1.15, 2.25]$ MeV	
$\varepsilon_c$ 2.2MeV $\gamma$ energy $E > 0.2$ MeV	0.563
$\varepsilon_c$ $^{11}\text{C}$ -2.2MeV $\gamma$ distance $d < 0.35$ m	
Total	0.360

production rate is computed from:

$$R(^{11}\text{C}) = \frac{A}{\frac{4}{3}\pi r^3 \rho T} \cdot \frac{1}{\varepsilon_{vis} \cdot \varepsilon_{end} \cdot \varepsilon_t \cdot \varepsilon_{escape} \cdot \varepsilon_c} \quad (4)$$

$$= 0.130 \pm 0.026(\text{stat}) \pm 0.014(\text{syst}) \text{day}^{-1} \text{ton}^{-1}$$

( $A = 54 \pm 11$ ,  $b \times T_w = 164 \pm 15$  and  $\chi^2/\text{d.o.f} = 9.7/13$ ) where  $r$  is the selected volume radius (0.8 m),  $\rho$  the scintillator

density (0.88 g/cm<sup>3</sup>) and  $T$  the detector live time (611 days). All the efficiencies in Eq 4 are reported in Table I.

The systematic error has been derived by propagating the uncertainties of the reconstruction position ( $\sim 1.5\%$ ) and of the light yield ( $\sim 8.5\%$ ) in Eq 4. The systematics takes also into account the stability of the result when the cut parameters vary around the optimal values.

The analysis measured rate is in good agreement with the expected one from the CERN experiment:  $0.146 \pm 0.015 \text{day}^{-1} \text{ton}^{-1}$ .

## VII. DISCUSSION

The success of the three-fold coincidence technique in selecting  $^{11}\text{C}$  events and in evaluating correctly their production rate is promising in prospective of deep underground liquid scintillator detectors.

The expected rates for  $pep$  and CNO neutrinos in Borexino are  $0.021$  and  $0.035 \text{day}^{-1} \text{ton}^{-1}$  (BP2004+LMA+LUNA [18, 19, 20]), respectively. In the energy range of observation [0.8,1.3] MeV, beyond the  $^7\text{Be}-\nu$  electron recoil energy spectrum, the  $pep$ +CNO signal,  $S_\nu$ , is reduced to  $0.015 \text{day}^{-1} \text{ton}^{-1}$ . In the same window, the expected contamination from  $^{11}\text{C}$  is then about 5 times higher ( $B_{^{11}\text{C}} = 0.074 \pm 0.008 \text{day}^{-1} \text{ton}^{-1}$ ).

A second background contribution arises from the trace contaminants in the scintillator mixture. Assuming for the  $^{238}\text{U}$  and  $^{232}\text{Th}$  a concentration level of  $10^{-17}\text{g/g}$  and  $10^{-15}\text{g/g}$  for the  $^{nat}\text{K}$ , the non-cosmogenic contaminants,  $B_{n.c.}$ , contribute to the  $pep$ +CNO window with  $0.006 \text{day}^{-1} \text{ton}^{-1}$ .

In order to reach a signal-to-background ratio equal to 1, the detection efficiency of Borexino must be larger than  $1 - S_\nu/(B_{^{11}\text{C}}+B_{n.c.}) = 0.81$ . The detection efficiency is limited by the physics ( $^{12}\text{C}(X,Y)^{11}\text{C}$  invisible channels), by the detector itself (low energy threshold and dead time between sequential triggers) and by the software cuts in time and space around the neutron capture  $\gamma$ 's. Since, in fact, the three fold coincidence does not identify the single  $^{11}\text{C}$  decay but localizes it in a spherical volume  $V_{^{11}\text{C}}$ , the entire volume  $V_{^{11}\text{C}}$  must be discarded for a time equivalent to few  $^{11}\text{C}$  lifetimes. Thus, the main challenge will be the minimization of the detector mass-time fraction loss.

Assuming a neutron rate of  $1.5 \times 10^{-2} \mu^{-1} \text{m}^{-1}$  [7, 21], we estimate that, even including the trace contamination, Borexino can reach a signal-to-background ratio equals to 1, losing only 14% of the data [7, 22]. The optimal cuts and the relative efficiencies expected for Borexino are quoted in Table II.

Furthermore, the Borexino collaboration is investigating [23] the possibility to improve the three-fold coincidence technique by exploiting the muon track: the reconstruction of the muon track leads, in fact, to the definition of a cylindrical volume around the track itself. Intersecting the cylindrical volume with the spherical one centered on the 2.2MeV $\gamma$ , Borexino can efficiently remove  $^{11}\text{C}$  events while reducing significantly the fraction of data loss.

TABLE II: Predicted  $^{11}\text{C}$  decay detection efficiencies for the Borexino detector in order to reach a signal ( $pep+\text{CNO } \nu\text{s}$ ) to background ( $^{11}\text{C}$  decays) ratio equal to 1. The trace contamination is assumed at the level of  $10^{-17}$  g/g for  $^{238}\text{U}$  and  $^{232}\text{Th}$  and  $10^{-15}$  g/g for  $^{nat}\text{K}$ .

Efficiency	Reason	Value
$\varepsilon_{vis}$	visible channels	0.955
$\varepsilon_t$	$\mu\text{-}2.2\text{MeV}\gamma$ coincidence	0.989
$\varepsilon_c$	$2.2\text{MeV}\gamma$ energy $E > 0.2$ MeV	0.954
$\varepsilon_d$	$^{11}\text{C}\text{-}2.2\text{MeV}\gamma$ distance $d < 1$ m	0.984
$\varepsilon_t$	$^{11}\text{C}\text{-}2.2\text{MeV}\gamma$ coincidence time $T < 5 \times \tau_{^{11}\text{C}}$	0.993
Total		0.880

### VIII. CONCLUDING REMARKS

In this paper we presented the results of the cosmogenic  $^{11}\text{C}$  measurement based on the three-fold coincidence technique with the Borexino Counting Test Facility. For the first time, deep underground  $^{11}\text{C}$  production has been detected *in situ* event by event.

The agreement between the measured  $^{11}\text{C}$  production rate observed in CTF and the value extrapolated from the measurement performed at the NA54 CERN facility in a muon on target experiment [10], demonstrated that the three-fold coinci-

dence technique is a powerful tool for isolating and discriminating the  $^{11}\text{C}$  background.

The results also indicate an agreement with the theoretical calculation in [7]. When combined with the prediction that the overall rate of  $^{11}\text{C}$  produced without free neutrons in the final state is limited at 4.5%, this observation indicated that Borexino should be able to minimize the  $^{11}\text{C}$  background at a level compatible with the observation of  $pep$  neutrinos.

In perspective of Borexino, such result opens a new window in  $pep$  and CNO neutrino spectroscopy.

### IX. ACKNOWLEDGEMENTS

We thank D. Motta and E. Resconi for the useful discussions and comments and I. Manno, L. Cadonati, M. Goeger-Neff, A. Sonnenschein, A. Di Credico and G. Testera for their past contributions.

This work has been supported in part by the Istituto Nazionale di Fisica Nucleare, the Deutsche Forschungsgemeinschaft (DFG, Sonderforschungsbereich 375), the German Bundesministerium für Bildung und Forschung (BMBF), the Maier-Leibnitz-Laboratorium (Munich), the Virtual Institute for Dark Matter and Neutrino Physics (VIDMAN, HGF) and the U.S. National Science Foundation under grants PHY-0201141, PHY-9972127 and PHY-0501118.

- 
- [1] Homestake Collaboration, B. T. Cleveland *et al.*, *Astrophys. J.* **496**, 505 (1998); SAGE Collaboration, J. N. Abdurashitov *et al.*, *J. Exp. Theor. Phys.* **95**, 181 (2002); GNO Collaboration, M. Altmann *et al.*, *Phys. Lett. B* **616**, 174 (2005); T. Nakaya [Super-Kamiokande Collaboration], eConf C020620, SAAT01 (2002); SNO Collaboration, Q. R. Ahmad *et al.*, *Phys. Rev. Lett.* **89**, 011301 (2002); SNO Collaboration, Q.R. Ahmad *et al.*, *Phys. Rev. Lett.* **89**, 011302 (2002).
- [2] KamLAND Collaboration, K. Eguchi *et al.*, *Phys. Rev. Lett.* **90**, 21802 (2003).
- [3] J. N. Bahcall and M. H. Pinsonneault, *Rev. Mod. Phys.* **64**, 885 (1992)
- [4] J. N. Bahcall and C. Peña-Garay, *New J. Phys.*, **6**, 63 (2004).
- [5] G. Imbriani *et al.*, astro-ph/0403071 (2005).
- [6] M. Deutsch, *Proposal for a Cosmic Ray Detection System for the Borexino Solar Neutrino Experiment*, Massachusetts Institute of Technology, 1996.
- [7] C. Galbiati *et al.*, *Phys. Rev. C* **71**, 055805 (2005).
- [8] Borexino Collaboration, G. Alimonti *et al.*, *Nucl. Instr. Meth. A* **406**, 411 (1998).
- [9] Borexino Collaboration, G. Alimonti *et al.*, *Astropart. Phys.*, **8**, 141 (1998).
- [10] T. Hagner *et al.*, *Astropart. Phys.* **14**, 33 (2000).
- [11] Borexino Collaboration, G. Alimonti *et al.*, *Astropart. Phys.* **16**, 205 (2002).
- [12] MACRO Collaboration, M. Ambrosio *et al.*, *Astropart. Phys.* **10**, 11 (1999); MACRO Collaboration, M. Ambrosio *et al.*, *Astropart. Phys.* **19**, 313 (2003);
- [13] A. Fassò *et al.*, *Electron-photon transport in FLUKA: Status*, Proceedings of the MonteCarlo 2000 Conference, Lisbon, October 23-26 2000; A. Kling, F. Barao, M. Nakagawa, L. Tavora and P. Vaz eds., Springer-Verlag Berlin, p. 159 (2001); A. Fassò *et al.*, FLUKA: *Status and Prospective for Hadronic Applications*, Proceedings of the MonteCarlo 2000 Conference, Lisbon, October 23-26 2000; A. Kling, F. Barao, M. Nakagawa, L. Tavora and P. Vaz eds., Springer-Verlag Berlin, p. 955 (2001).
- [14] P.G. Catalano *et al.*, *Mem. Soc. Geol. It.*, **35** 647 (1986).
- [15] D. Franco *The Borexino Experiment: Test of the Purification Systems and Data Analysis in the Counting Test Facility.*, Ph.D. Thesis, Università degli Studi di Milano and University of Heidelberg, 2005, <http://www.ub.uni-heidelberg.de/archiv/5403>.
- [16] D. D'Angelo *Toward the detection of low energy solar neutrinos in Borexino: data readout, data reconstruction and background identification*, Ph.D. Thesis, Technische Universität München, 2005.
- [17] Borexino Collaboration, G. Alimonti *et al.*, *Nucl. Instr. Meth. A*, **440**, 360 (2002).
- [18] J. N. Bahcall and M. H. Pinsonneault, *Phys. Rev. Lett.* **92**, 121301 (2004).
- [19] A. Formicola *et al.*, *Phys. Lett. B* **591**, 61 (2004).
- [20] J. N. Bahcall and C. Peña-Garay, *JHEP* 0311 004, (2003).
- [21] LVD Collaboration, M. Aglietta *et al.*, *Proc. 26th Inter. Cosmic Ray Conf.*, Vol. 2, 44 (1999), hep-ex/9905047.
- [22] D. Franco for the Borexino Collaboration, *Nucl. Phys. Proc. Suppl.* **145**, 29 (2005).
- [23] M. Chen, *Muon Veto Supplement Proposal for the Borexino Experiment*, editor. National Science Foundation Princeton University, Apr 1998.